Experimental Investigation of the Combustion Properties of a Representative Thermal Runaway Gas from Li-Ion Batteries

Olivier Mathieu, Mattias A. Turner, Darryl J. Mohr, James C. Thomas, and Eric L. Petersen
J. Mike Walker '66 Department of Mechanical Engineering, Texas A&M University
College Station, Texas, USA

1 Introduction

Lithium-Ion batteries are used in most electronic devices as well as in electric vehicles. As the proportion of electric vehicles on the road is rapidly increasing in many countries, more and more collisions involving these vehicles are to be expected. In case of severe collision, the battery can be crushed or penetrated which can lead to a short circuit (electric abuse) and eventually to thermal abuse and thermal runaway when the reactive electrolyte (a mixture of linear and cyclic carbonates, essentially) reacts due to the heat [1]. As the electrolyte reacts (a pyrolysis process, essentially), flammable gases are created which can lead to a fire if the hot flammable gases vent to the air. Thermal runaway gases (TRG) from Li-ion batteries have been characterized in many studies [2], but their combustion properties have never been investigated at the fundamental combustion level. One of the reasons behind that is due to the fact that the TRG composition varies with the electrolyte composition, the nature of the electrode, the state of charge of the battery, the failure environment (air, N_2, vacuum…), etc. [2,3].

However, despite this large number of factors influencing the TRG composition, it is worth mentioning that the detected species are very similar between studies, although their specific concentrations can vary greatly. In the present study, we assembled the detailed composition of the vent gases from the studies listed in [2] and in [3], and forty compositions were identified. An average mixture was determined from these forty compositions, and a few assumptions were made: the O_2 and N_2 concentration were disregarded, as they most likely essentially come from air; no vaporized battery electrolytes were taken into account as only one study detected them [4]; and their combustion properties are not well-known (some linear carbonates) or not known at all (cyclic carbonates), so they need to be studied separately. Finally, the components with too low of an average concentration (C_2H_2 and C_3H_6) are not likely to make any difference on the combustion properties of the final mixture, and these were excluded. The final mixture is composed of seven components and is defined in Table 1. As one can see, all the fuels listed in this table have been studied extensively. However, to the best of our knowledge, such a complex mixture of these gases was never investigated before. Note also the large proportion of CO_2 which, while inert, can pose a challenge to kinetics mechanisms when used as a diluent, even for very simple mixtures, at least at high pressure [5]. The mixture studied herein is therefore a great way to assess the accuracy of the base chemistry of detailed kinetics mechanisms available in the literature. To do so, ignition delay times and laminar flame speeds were measured in a shock tube and in a closed

Correspondence to: olivier.mathieu@tamu.edu

vessel, respectively. The fuel/air mixtures were studied at (flame speed) or close to (ignition delay time) atmospheric pressure. The following models were used for comparison with the data and assessment: GRI3.0 [6], JetSurfII [7], AramcoMech 1.3 [8], CRECK2003 [9], and NUIG 1.1 [10].

Table 1: Li-ion battery thermal runaway gas mixture used during this study.

Fuel	C_3H_8	C_2H_6	C_2H_4	CH_4	H_2	CO	CO_2
Mole fraction	0.007	0.019	0.027	0.119	0.144	0.168	0.516

2 Experimental methods

2.1 Shock tube and ignition delay time measurements

Ignition delay time measurements of the TRG mixture were performed in a single-diaphragm (polycarbonate, 0.25-mm thickness), stainless-steel shock tube (15.24-cm i.d., 4.72-m long and 7.62-cm i.d., 2.46-m long for the driven and driver sections, respectively). Five PCB-113B22 piezoelectric pressure transducers were used to measure the velocity of the incident shock wave, which was extrapolated to the endwall to determine post reflected-shock conditions. Using this method, the uncertainty in the temperature behind reflected shock waves (T_5) is maintained below 10 K. Test pressure was monitored by one Kistler 603-B1 transducer located on the sidewall (16 mm from the endwall), and one PCB-113B22 transducer on the endwall. At both these locations, OH* signals were recorded using an interference filter at 307 ± 10 nm. The test section was evacuated to 2×10^{-5} Torr or better using a roughing pump and a turbomolecular pump before each experiment. The ignition delay time was measured using the OH* signal from the endwall with the endwall pressure signal to determined time zero, Fig. 1. The uncertainty in these measurements is estimated to be about 10%. Test mixtures were prepared manometrically in a stainless-steel mixing tank. The gas purities were the following: H_2, Air (premixed, certified 21% O_2, 79% N_2) (Praxair, 99.999%), CH_4 (Praxair, 99.97%), C_2H_4 (Praxair, 99.995 %), C_2H_6, (Acetylene Oxygen Company, 99.5%), C_3H_8 (Praxair, 99.5%), CO (Praxair, 99.9%), and CO_2 (Praxair, 99.99%).

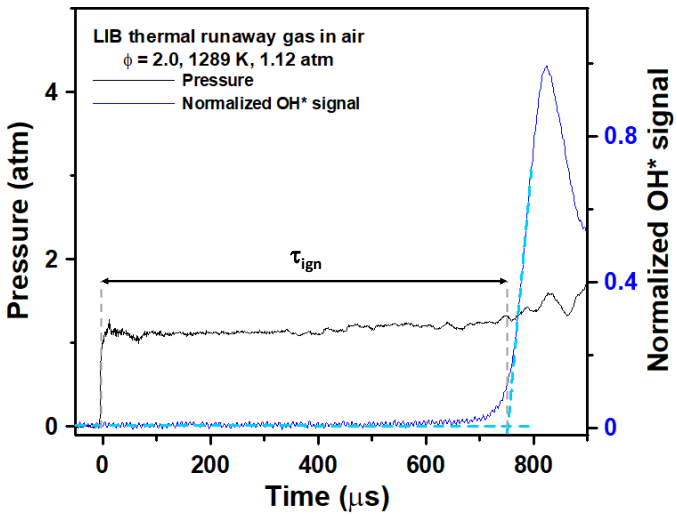

Figure 1: Determination method for the ignition delay time.

2.2 Closed vessel and laminar flame speed measurements

Spherically expanding flame experiments were conducted using a cylindrical chamber with approximately 34 L of internal volume. The chamber is equipped with opposed, 12.7-cm diameter windows, providing optical access to a schlieren diagnostic. Flame-front-tracking software was developed in-house to extract flame radii from the schlieren images using contrast adjustment and Canny edge detection. The rate of change of the flame radius is determined from the time history of the flame radius. The propagation speed of the flame relative to the burned gas was extrapolated to its unstretched value using Eq. 1, which is a nonlinear relationship between the burned flame speed and the stretch rate of the flame described originally by Markstein [11], investigated by Frankel and Sivashinsky [12], and analyzed in detail by Chen [13]. For spherically expanding flames with positive or near-zero Markstein lengths, Eq. 1 is highly accurate [13]. To arrive at the unstretched, unburned flame speed, continuity is applied in Eq. 2, where the burned-gas speed is multiplied by the ratio of the densities of the burned and unburned gases. More detail on this analysis process is given by Sikes et al. [14].

$$S_b = S_b^0 - S_b^0 L_{M,b} \frac{2}{r} \quad (1)$$

$$S_L^0 = \sigma S_b^0 \quad (2)$$

In Eq. 1, $L_{M,b}$ refers to the burned-gas Markstein length, and r refers to the radius of the flame. The mixture densities were calculated using AramcoMech 1.3 [8] and the equilibrium chemistry routine in Chemkin-Pro. A large batch of fuel mixture (Table 1) was prepared manometrically in a stainless-steel mixing tank, and this mixture was mixed with air at the desired equivalence ratio directly in the flame-speed vessel prior to each experiment.

3 Results and Comparison with Models

3.1 Ignition delay time measurements

The ignition delay time results are visible in Fig. 2. The comparison between the equivalence ratios (ϕ) investigated, Fig. 2(a), shows a large effect of the equivalence ratio on the ignition delay time. Increasing the equivalence ratio from 0.5 to 1.0 increases the ignition delay time from between a factor of about 2 (high temperature) and 1.5 (high temperature). Similar factors are observed when increasing ϕ from 1.0 to 2.0. For the fuel-lean results, (Fig. 2(b)) the comparison with the models show that the models considered herein are relatively accurate and within the experimental uncertainty above 1250 K but tend to underpredict ignition delay time. Below this temperature, it is interesting to observe that the two oldest models considered herein are very close to the data (the GRI3.0 model being the closest to this set of data overall), whereas the modern mechanisms over-predict the increase of the delay as the temperature decreases by 33% (NUIG 1.1 and CRECK 2003) or higher (Aramcomech 1.3).

For the stoichiometric condition (Fig. 2(c)), the GRI3.0 mechanism is this time the least accurate and predicts ignition delay times that are too short by a factor of about 1.5-2.0 but presents an activation energy that is close to the data. The JetSurf II model is closer to the data on the colder-temperature side, and the three recent models are close to the data overall but tend to over-predict the activation energy. For the fuel-rich data (Fig. 2(d)), the prediction difference amongst the models is larger, and the NUIG 1.1 model is the only one that is relatively accurate in predicting the data. The other models present an over-reactivity (too short of an ignition delay time), especially for the JetSurf II and GRI3.0 models.

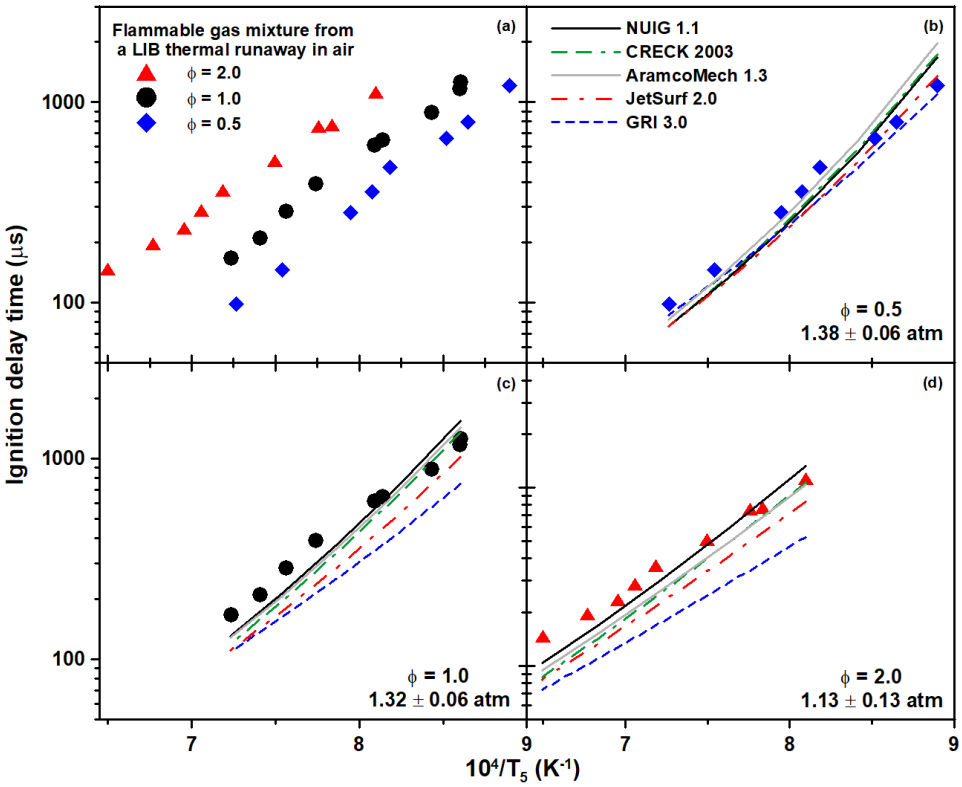

Figure 2: Ignition delay times of a mixture representative of thermal runaway gases from a Li-ion battery (Table 1) at various equivalence ratios and comparisons with models from the literature.

3.2 Laminar flame speed measurements

As can be seen in Fig.3, the laminar flame speed of the TRG mixture presents the classical shape observed with hydrocarbons and passes by a maximum (23.25 cm/s) at an equivalence ratio of around 1.1, also like most hydrocarbons. Concerning the models, only the CRECK and, to a lesser extent, NUIG 1.1 and AramcoMech 1.3 models are able to reproduce the data with high accuracy. The GRI3.0 model is the only one that over-predicts the data (over the entire range of equivalence ratios investigated) by about 7.5% at the peak value. The other model considered (JetSurfII) tends to under-estimate the flame speed above $\phi = 0.9$, by up to about 5%, the experimental uncertainty being estimated to be below 3% [14].

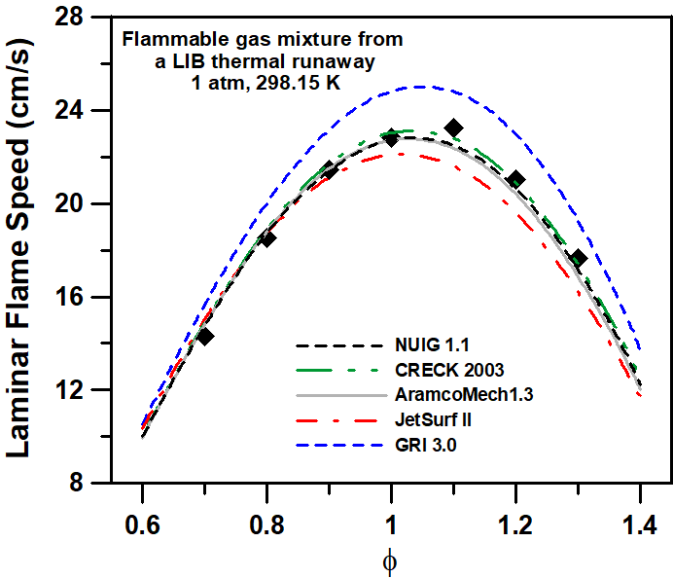

Figure 3: Laminar flame speeds of a flammable gas mixture representative of the gases formed during a thermal runaway from a Li-ion battery (Table 1) in air at 1 atm and an initial temperature of 298 K.

4 Conclusion

An average mixture of vent gases from the thermal runaway of Lithium-ion batteries was determined based on forty different mixtures. The final mixture contains seven components, and the combustion of this complex mixture was investigated in a shock tube (ignition delay time) and closed vessel (laminar flame speed) in air. Results were compared to detailed kinetics mechanisms from the literature. Recent detailed kinetics mechanisms can predict the data with high accuracy, with the most recent one (NUIG 1.1) being the most accurate overall. The complexity of the present mixture, investigated for the first time, will allow for further improvement of the models in the future.

5 Acknowledgments

The authors would like to thank the National Science Foundation for the financial support of this study (award # 2037795). Additional support came from the TEES Turbomachinery Laboratory.

References

[1] Wang Q, Mao B, Stoliarov SI, Sun J. (2019). A review of lithium ion battery failure mechanisms and fire prevention strategies. Progress in Energy and Combustion Science 73: 95.

[2] Baird AR, Archibald EJ, Marr KC, Ofodike A. Ezekoye OA. (2020). Explosion hazards from lithium-ion battery vent gas. Journal of Power Sources 446: 227257.

[3] Spray R, Barry M, Vickery J, Myers T. (2020). Understanding how testing conditions affect hazard quantification in Lithium-ion battery abuse tests. NASA Aerospace Battery Workshop (Virtual). Available at (last consulted on 08/20/2021): https://www.nasa.gov/sites/default/files/atoms/files/nabw20_how_test_cond_affect_haz_quan_li-ion_batt_abuse_test_rspray.pdf.

[4] Fernandes Y, Bry A, de Persis S. (2018). Identification and quantification of gases emitted during abuse tests by overcharge of a commercial Li-ion battery. J. Power Sources 389: 106.

[5] Barak S, Ninnemann E, Neupane S, Barnes F, Kapat J, Vasu S. (2019). High-Pressure Oxy-Syngas Ignition Delay Times With CO_2 Dilution: Shock Tube Measurements and Comparison of the Performance of Kinetic Mechanisms. J. Eng. Gas Turbines Power. 141: 021011.

[6] Smith GP, Golden DM, Frenklach M, Moriarty NW, Eiteneer B, Goldenberg M, Bowman CT, Hanson RK, Song S, Gardiner WC, Lissianski VV, Qin Z. (1999), available at: http://www.me.berkeley.edu/gri_mech/

[7] Wang H, Dames E, Sirjean B, Sheen DA, Tango R, Violi A, Lai JYW, Egolfopoulos FN, Davidson DF, Hanson RK, Bowman CT, Law CK, Tsang W, Cernansky NP, Miller DL, Lindstedt RP. (2010). A high-temperature chemical kinetic model of n-alkane (up to n-dodecane), cyclohexane, and methyl-, ethyl-, n-propyl and n-butyl-cyclohexane oxidation at high temperatures. JetSurF version 2.0, available at: (http://web.stanford.edu/group/haiwanglab/JetSurF/JetSurF2.0/index.html).

[8] Metcalfe WK, Burke SM, Ahmed SS, Curran HJ. (2013). A Hierarchical and Comparative Kinetic Modeling Study of C1 − C2 Hydrocarbon and Oxygenated Fuels. Int. J. Chem. Kinet. 45: 638.

[9] Ranzi E, Cavallotti C, Cuoci A, Frassoldati A, Pelucchi M, Faravelli T. (2015). New reaction classes in the kinetic modeling of low temperature oxidation of n-alkanes. Combust. Flame, 162: 1679. Available at: http://creckmodeling.chem.polimi.it/menu-kinetics/menu-kinetics-detailed-mechanisms

[10] Baigmohammadi M, Patel V, Nagaraja S, Ramalingam A, Martinez S, Panigrahy S, Mohamed A, Somers KP, Burke U, Heufer KA, Pekalski A, H.J. Curran HJ. (2020). Comprehensive experimental and simulation study of the ignition delay time characteristics of binary blended methane, ethane, and ethylene over a wide range of temperature, pressure, equivalence ratio, and dilution. Energy Fuels 34: 8808.

[11] Markstein GH. (1951). Experimental and Theoretical Studies of Flame-Front Stability. J. Aero. Sci. 18: 199.

[12] Frankel ML, Sivashinsky GI. (1983). On Effects Due To Thermal Expansion and Lewis Number in Spherical Flame Propagation. Combust. Sci. Technol. 31: 131.

[13] Chen Z. (2011). On the extraction of laminar flame speed and Markstein length from outwardly propagating spherical flames. Combust. Flame 158: 291.

[14] Sikes T, Mannan MS, Petersen EL. (2018). An experimental study: laminar flame speed sensitivity from spherical flames in stoichiometric CH_4–air mixtures. Combust. Sci. Technol. 190: 1594.